Published in final edited form as:
Exp Neurol. 2014 April ; 254: 180–189. doi:10.1016/j.expneurol.2014.01.020.

SN79, a sigma receptor antagonist, attenuates methamphetamine-induced astrogliosis through a blockade of OSMR/gp130 signaling and STAT3 phosphorylation

Matthew J. Robson[1,2], **Ryan C. Turner**[3,4], **Zachary J. Naser**[3], **Christopher R. McCurdy**[5], **James P. O'Callaghan**[6], **Jason D. Huber**[1,4], and **Rae R. Matsumoto**[1,4]

[1]Department of Basic Pharmaceutical Sciences, School of Pharmacy, West Virginia University 1 Medical Center Dr., West Virginia University Health Sciences Center Morgantown, WV 26506

[2]Department of Pharmacology, School of Medicine, Vanderbilt University 1161 21st Ave S. Nashville, TN 37232

[3]Department of Neurosurgery, School of Medicine, West Virginia University 1 Medical Center Dr., West Virginia University Health Sciences Center Morgantown, WV 26506

[4]Center for Neuroscience, School of Medicine, West Virginia University 1 Medical Center Dr., West Virginia University Health Sciences Center Morgantown, WV 26506

[5]Department of Medicinal Chemistry and Department of Pharmacology, School of Pharmacy University of Mississippi P.O. Box 1848 University, MS 38677-1848

[6]Health Effects Laboratory Division, Centers for Disease Control and Prevention, National Institute of Occupational Safety and Health 1095 Willowdale Rd. Morgantown, WV 26505

Abstract

Methamphetamine (METH) exposure results in dopaminergic neurotoxicity in striatal regions of the brain, an effect that has been linked to an increased risk of Parkinson's disease. Various aspects of neuroinflammation, including astrogliosis, are believed to be contributory factors in METH neurotoxicity. METH interacts with sigma receptors at physiologically relevant concentrations and treatment with sigma receptor antagonists has been shown to mitigate METH-induced neurotoxicity in rodent models. Whether these compounds alter the responses of glial cells within the central nervous system to METH however has yet to be determined. Therefore, the purpose of the current study was to determine whether the sigma receptor antagonist, SN79, mitigates METH-induced striatal reactive astrogliosis. Male, Swiss Webster mice treated with a neurotoxic regimen of METH exhibited time-dependent increases in striatal *gfap* mRNA and concomitant increases in GFAP protein, indicative of astrogliosis. This is the first report that similar to other neurotoxicants that induce astrogliosis through the activation of JAK2/STAT3 signaling by

Corresponding author: Rae R. Matsumoto, West Virginia University, School of Pharmacy, 1 Medical Center Drive, Morgantown, WV 26506. Phone: 1-304-293-1450; FAX: 1-304-293-2576. rmatsumoto@hsc.wvu.edu.

stimulating gp-130-linked cytokine signaling resulting from neuroinflammation, METH treatment also increases astrocytic oncostatin m receptor (OSMR) expression and the phosphorylation of STAT3 (Tyr-705) *in vivo*. Pretreatment with SN79 blocked METH-induced increases in OSMR, STAT3 phosphorylation and astrocyte activation within the striatum. Additionally, METH treatment resulted in striatal cellular degeneration as measured by Fluoro-Jade B, an effect that was mitigated by SN79. The current study provides evidence that sigma receptor antagonists attenuate METH-induced astrocyte activation through a pathway believed to be shared by various neurotoxicants.

Keywords

sigma receptor; methamphetamine neurotoxicity; glia; astrocyte; neuroinflammation

INTRODUCTION

Methamphetamine (METH) is an illicit substance that acts as an addictive psychostimulant by modulating monoamine signaling within the central nervous system (CNS). Chronic METH abuse results in several negative side effects, including dopaminergic nerve terminal toxicity (Romanelli and Smith 2006; Volkow et al. 2001a; Volkow et al. 2001b), altered morphology in the substantia nigra (Todd et al. 2013), and an increased risk of developing Parkinson's disease later in life (Callaghan et al. 2010; Callaghan et al. 2012). Many of these effects have been replicated in various animal models, including recent reports showing that significant METH-induced neurotoxicity occurs in rodents who self-administer the drug (Reichel et al. 2012; Schwendt et al. 2009).

In addition to having dramatic effects on dopaminergic neurons, METH affects a variety of other cell types located within the CNS (Cadet and Krasnova 2009), including astrocytes in regions of the brain affected by its neurotoxic actions (Bowyer et al. 1994; O'Callaghan and Miller 1994; Pu et al. 1994). Astrocytes isolated from regions of the brain affected by the toxic effects of METH appear more sensitive to the effects of the drug than comparable cell populations from other areas (Lau et al. 2000; Stadlin et al. 1998). *In vitro* studies using isolated astrocytes have confirmed that METH can directly exert actions on these cells; however, it is currently unclear whether *in vivo* activation of astrocytes by METH also results from direct actions on this cell type or whether it is a consequence of neuronal damage and neuroinflammation (Hebert and O'Callaghan 2000; Kelly et al. 2012; Lau et al. 2000; Narita et al. 2006; Sriram et al. 2004; Stadlin et al. 1998).

Astrocytes are activated in response to a variety of CNS insults through a process termed astrogliosis whereby they undergo distinct morphological changes and display an increase in the expression of glial fibrillary acidic protein (GFAP) (Raivich et al. 1999). One mechanism by which astrocytes can be activated is through the induction of STAT3 phosphorylation through JAK/STAT signaling events (Hebert and O'Callaghan 2000). It is hypothesized that this phosphorylation occurs through gp130-mediated cytokine signaling events initiated by inflammatory processes (Hebert and O'Callaghan 2000; Van Wagoner and Benveniste 1999). The phosphorylation and therefore activation of STAT3 in astrocytes

can be mediated through oncostatin M (OSM)-mediated signaling through the oncostatin M receptor (OSMR) (Van Wagoner et al. 2000). OSMR is an IL-6-type cytokine receptor that dimerizes with gp130 and mediates intercellular signaling events, including STAT3 (Tyr-705) phosphorylation (Chen and Benveniste 2004; Van Wagoner et al. 2000). Interestingly, OSM signaling through OSMRβ/gp130 is believed to modulate astrocyte function and the expression of GFAP is decreased in mice deficient in gp130 (Chen et al. 2006; Nakashima et al. 1999), providing evidence that signaling through OSMRβ/gp130 complexes is involved in GFAP upregulation and subsequent astrogliosis. Furthermore, METH results in increased expression of *osmr* and *gfap* in regions of the brain affected by the neurotoxic effects of the drug in rodents (Thomas et al. 2004). There is, however, a paucity of studies confirming the effect of METH on the transcriptional regulation of *osmr* in astrocytes per se, although a recent report has shown that *osmr* expression increases in astrocytes activated *in vivo* by other insults, such as ischemic stroke or peripheral lipopolysaccharide (LPS) injections (Zamanian et al. 2012).

Exacerbating the problem of METH-induced neurotoxicity is the current lack of FDA approved pharmacotherapies for treating the negative health effects of METH usage. One potentially promising molecular target for the production of medications aimed at counteracting these effects are sigma receptors. There are currently two known subtypes of sigma receptors (Hellewell and Bowen 1990). METH interacts with both subtypes of sigma receptors, denoted sigma-1 and sigma-2 receptors, at physiologically relevant concentrations and sigma receptor antagonists have been shown to mitigate the neurotoxic effects of METH on dopaminergic and serotonergic systems within the CNS (Kaushal et al. 2013; Matsumoto et al. 2008; Nguyen et al. 2005). Sigma receptors are expressed in astrocytes and sigma receptor modulation has been shown to modulate the activity of astrocytes both *in vitro* and *in vivo* (Ajmo et al. 2006; Klouz et al. 2003); however whether sigma receptor modulation alters METH-induced astrocyte activation has yet to be determined.

Therefore, the primary purpose of the current study was to determine if the putative sigma receptor antagonist, SN79 (6-acetyl-3-(4-(4-(4-fluorophenyl)piperazin-1-yl)butyl)benzo[d]oxazol-2(3H)-one), mitigates METH-induced reactive astrogliosis and cellular degeneration in the striatum. SN79 has been shown in earlier studies to attenuate a number of METH-induced effects including microglial activation (Robson et al. 2013) and other classical striatal dopaminergic and serotonergic deficits which are similarly mitigated by other sigma receptor antagonists (Kaushal et al. 2011b; Seminerio et al. 2012a; Seminerio et al. 2011). Secondly, we wanted to determine if sigma receptor modulation results in a blockade of OSMRβ/gp130-induced STAT3 phosphorylation which has been implicated in the activation of astrocytes following CNS insults. Herein, we provide evidence that METH treatment results in an increase in OSMR expression and signaling through STAT3 in astroctyes with subsequent reactive astrogliosis, effects mitigated by treatment with the sigma receptor antagonist and potential drug development candidate, SN79.

MATERIALS AND METHODS

Drugs and chemicals

(+)-Methamphetamine hydrochloride was obtained from Sigma Aldrich (St. Louis, MO). SN79 (6-acetyl-3-(4-(4-(4-fluorophenyl)piperazin-1-yl)butyl)benzo[d]oxazol-2(3H)-one) was synthesized as previously described (Kaushal et al. 2011a) and provided by Dr. Christopher R. McCurdy (University of Mississippi, University, MS). Compared to other sigma receptor antagonists, SN79 has a favorable pharmacokinetic profile that makes it a promising drug development lead (Kaushal et al. 2011a). All drugs administered to animals were dissolved in sterile saline solution (0.1 mL/10 g body weight) (Teknova, Fisher Scientific, Pittsburgh, PA). All other chemicals were obtained from Sigma Aldrich (St. Louis, MO) unless otherwise specified.

Animals

Male, Swiss Webster mice (24-28 g; Harlan, Indianapolis, IN) were utilized. Mice were housed in groups of five, on a 12:12 h light/dark cycle with food and water *ad libitum*. Mice were randomly assigned to their respective treatment groups. All experiments were performed as approved by the Animal Care and Use Committee at West Virginia University.

Repeated dosing paradigm

Mice were randomly distributed for each experiment into one of four treatment groups: 1) Saline/Saline (0.1 mL/10 g body weight), 2) Saline/METH 5 mg/kg, 3) SN79 3 mg/kg/ Saline, or 4) SN79 3 mg/kg/METH 5 mg/kg. The first compound listed in each pair (Saline or SN79) was administered intraperitoneally (i.p.) as a pretreatment 15 min prior to the second compound in each treatment group (Saline or METH, i.p.). Each animal underwent four pretreatments/treatments at 2 h apart as previously described (Kaushal et al. 2013).

The METH dose (5 mg/kg × 4) was selected based upon previous dose response experiments, where it consistently produced significant dopaminergic deficits in the striatum in this specific model (Matsumoto et al. 2008; Seminerio et al. 2012a). The dose of SN79 (3 mg/kg × 4) was selected based on previously reported dose response experiments assessing the ability of this compound to mitigate the striatal dopaminergic deficits elicited by METH treatment (Kaushal et al. 2013).

Quantitative real time PCR

At various time points post-treatment (as measured from the last injection), bilateral striatum samples were collected (n=10/treatment group from two distinct experiments), flash frozen in liquid nitrogen and stored at −80° C for later use. Total RNA was then extracted from flash frozen striatum samples using Trizol reagent (Invitrogen, Grand Island, NY) according to manufacturer's instructions. The total RNA concentration for each sample was quantified by spectral absorption, and the purity of the sample checked to confirm that the 260/280 ratio was in the range of 1.8-2.1. Samples of cDNA were prepared by reverse transcription using a high capacity reverse transcription kit (Applied Biosystems, Foster City, CA). Each sample reaction included MultiScribe TM Reverse Transcriptase and random primers, with

thermal cycler conditions set as follows: step 1 at 25° C for 10 min, step 2 at 37° C for 120 min, step 3 at 85° C for 5 s, and step 4 at 4° C for 10 min.

For PCR amplification, TaqMan® Universal PCR Master Mix and the following probes were obtained from Applied Biosystems (Foster City, CA): *18s* (Hs99999901_s1) for use as an endogenous control gene, *gfap* (Mm01253033_m1), and *osmr* (Mm00495424_m1). The reaction mixture was prepared according to the manufacturer's instructions, with the following thermal cycling conditions: initial holding at 50° C for 2 min required for optimal AmpErase® UNG activity, followed by a first denaturing step at 95° C for 10 min, then 45 cycles at 95° C for 15 s, and at 60° C for 1 min. Data from real-time PCR measurements were calculated using the ΔΔCt method. The threshold value was set at 0.2 and the threshold cycle (Ct value) of each gene was then normalized to 18s rRNA.

Immunofluorescence imaging

At 72 h post-treatment (after the last injection), animals were anesthetized and perfused transcardially with phosphate buffered saline (PBS) followed by 4% paraformaldehyde. The entire brain was removed and immediately placed in 4% paraformaldehyde for 24 h. Following fixation, the brains were processed using a Tissue-Tek VIP 5 automatic tissue processor (Sakura Finetek, Torrance, CA) and then embedded in paraffin with a Tissue-Tek TEC 5 embedding console system (Sakura Finetek). Embedded tissues were sliced in 6 μm sections using a Leica RM2235 microtome (Leica Microsystems, Buffalo Grove, IL), and slices mounted on glass slides for staining. All slides were heat-fixed and deparaffinized via a series of xylene and alcohol washes prior to immunofluorescent and immunohistochemistry procedures. Following deparaffinization and rehydration, endogenous peroxidases were quenched using a 10% methanol and 10% hydrogen peroxide solution in PBS for 30 min. Slides were permeabilized for 1 h using 1.8% L-lysine, 5% horse serum, and 0.1% Triton X-100 in Dulbecco's phosphate buffered saline (DPBS). Sections were then incubated in a polyclonal antibody raised in rabbit against anti-cow GFAP (DAKO, Glostrup, Denmark) at a dilution of 1:500 in 5% horse serum in PBS overnight at 4° C. Next, sections were washed twice for 10 min each in PBS prior to application of Alexa Fluor 488 goat anti-rabbit IgG (Invitrogen, Grand Island, NY) at a dilution of 1:100 in PBS for 3 h. Following the incubation in Alexa Fluor 488 goat anti-rabbit IgG, slides were rinsed twice for 10 min each in PBS. Then, the tissues were incubated with a polyclonal antibody raised in goat anti-mouse OSMR (LifeSpan Biosciences, Seattle, WA) at a dilution of 1:200 in 5% horse serum in PBS overnight at 4° C. Following the incubation in primary antibody, the slides were rinsed twice for 10 min each in PBS prior to the application of biotinylated anti-goat IgG (Vector Laboratories, Burlingame, CA) at a dilution of 1:10,000 in 5% horse serum in PBS for 2 h. Following the incubation in biotinylated anti-goat IgG, slides were rinsed twice for 10 min each in PBS prior to the application of Streptavidin Alexa Fluor 546 (Life Technology, Carlsbad, CA) at a dilution of 1:100 in PBS for 1 h. Slides were rinsed in PBS for 10 min and then coverslipped with Vectashield Mounting Media with 4’,6-diamidino-2-phenylindole (DAPI) (Vector Laboratories, Burlingame, CA). Finally, slides were sealed with acrylic and stored in the dark in a laboratory refrigerator at 4° C.

A total of three slices per brain were evaluated and averaged for each data point. Each experimental group comprised of n=5, with the animals being tested in two distinct experiments to ensure reproducibility of the data. Images were acquired using a Zeiss Axio Imager 2 microscope (Oberkocken, Germany) and quantified using ImageJ software (NIH; http://rsbweb.nih.gov/ij/) by analyzing fluorescence intensity as compared to background by splitting the multicolor image into each individual color and measuring the individual intensities of each cell body and processes compared to the background of the image. The separation of image for calculation was used to prevent the influence of one color onto another. Data were then transferred to GraphPad (San Diego, CA) for statistical comparison. In addition to fluorescent intensity quantification of GFAP and OSMR staining across treatment groups, colocalization analysis was completed using ImageJ as described previously (Bolte and Cordelieres 2006). Specifically, Pearson's coefficient and Manders' overlap coefficients were calculated. Values approaching 1 indicate increasing colocalization.

Immunohistochemistry imaging

For bright-field visualization of GFAP, slides were rinsed in DPBS, permeabilized with 1.8% L-lysine, 4% horse serum, and 0.2% Triton X-100 in DPBS. Sections were incubated overnight with a polyclonal antibody raised in rabbit against anti-cow GFAP (DAKO, Glostrup, Denmark) at a dilution of 1:500 in 4% horse serum in PBS. Sections were washed and incubated for 4 h in biotinylated anti-rabbit IgG (1:10,000) in PBS with 4% horse serum. Diaminobenzidine (DAB) was used as a chromogen following incubation in avidin D-horseradish peroxidase (HRP) for 1 h. Bright-field immunohistochemistry was quantified using stereology and the optical fractionator technique as previously described (Schmitz and Hof 2005; Smith et al. 2012; Turner et al. 2012). Briefly, a region of interest encompassing the striatum was drawn at low power using an Olympus AX70 microscope and accompanying StereoInvestigator software (MBF Bioscience, Williston, VT). Counting frames were randomly selected by the software and the cell-type of interest marked by an observer blinded to treatment. The volume of the region of interest previously identified was then determined by the software and the number of cells marked by the observer returned. Counting frames were 75 μm on each side with a depth of 6 μm.

In addition to nerve terminal damage, METH has been reported to result in striatal apoptosis and cellular toxicity *in vivo* (Deng et al. 2001; Jayanthi et al. 2005), which can be measured by Fluoro-Jade staining, a known marker of degeneration resulting from amphetamine treatment in rodents (Eisch et al. 1998; Schmued and Hopkins 2000). Fluoro-Jade labels degenerating neurons and activated glial cells including atrocytes (Anderson et al. 2003; Damjanac et al. 2007); the extent to which sigma receptor ligands mitigate METH-induced degeneration in the striatum has yet to be determined. For Fluoro-Jade B staining, sections were incubated in 0.06% potassium permanganate for 10 min, washed in deionized water, and incubated in 0.0004% Fluoro-Jade B in 0.1% acetic acid for 20 min. Sections were then washed, coverslipped, and sealed. Fluoro-Jade B was quantified using stereology and the optical fractionator technique as previously described (Schmitz and Hof 2005; Smith et al. 2012; Turner et al. 2012). A total of three slices per brain were evaluated and averaged for

each data point. Each experimental group comprised of n=5, with the animals being tested in two distinct experiments to ensure reproducibility of the data.

Immunoblotting

Twelve hours post-treatment (time from last treatment), animals were sacrificed utilizing focused microwave irradiation (Muromachi Microwave Applicator, TMW-4012C, 10 kW output) to preserve the phosphorylation states of proteins within each animal post-mortem, including STAT3 (Tyr-705) (O'Callaghan and Sriram 2004). Mice were briefly restrained in a water-jacketed holder and inserted into the machine head. The microwave beam was then activated (5 kW power setting for 1 s) and animals were subsequently removed from the holder. Brains were then removed and bilateral striatum samples dissected, flash frozen and stored at −80° C. Protein was isolated from each respective sample by sonication in 25 μL of hot (85-95° C) 1% sodium docecyl sulfate (SDS) as previously described (O'Callaghan and Sriram 2004). The protein concentration of each sample was measured using a Coomassie Plus Bradford Assay Kit (Pierce, Rockford, IL) which is based upon a modified form of the Bradford assay (Bradford 1976). Samples were run using 20 μg of protein/well using Tris-HCl 10% pre-cast 15-well gels (Bio-Rad, Hercules, CA) in combination with 5X Lammeli sample buffer. Gels were run using a mini-PROTEAN system (Bio-Rad) and gels were equilibrated for 15 min in Towbin's buffer prior to transfer to polyvinylidene fluoride (PVDF) membranes (Bio-Rad) using semi-dry electrophoretic transfer cells (Bio-Rad). Membranes were blocked using 5% fat-free milk/tris buffered saline and Tween 20 (TBS-T) for 2 h at room temperature. Membranes were incubated with primary phosphoSTAT3 (Tyr-705) or STAT3 antibody (Cell Signaling, Danvers, MA) at a concentration of 1:1000 overnight at 4° C. Anti-rabbit IgG HRP-linked antibody (Cell Signaling) was used as a secondary antibody at a concentration of 1:2000 with gentle shaking for 2 h. An HRP-conjugated β-actin rabbit monoclonal antibody (Cell Signaling) was used as an endogenous control for all samples at a concentration of 1:10,000 and incubated for 1 h. Molecular weight determination was conducted using a biotinylated protein ladder (Cell Signaling). Imaging was conducted using 20X LumiGLO chemiluminescent substrate (Cell Signaling) according to manufacturer's instructions. Images were converted to 8-bit and analyzed using densitometry with background subtraction and normalized to β-actin using ImageJ software (NIH; http://rsbweb.nih.gov/ij/).

Statistical Analysis

Statistical analyses were conducted using either one-way or two-way analysis of variance (ANOVA), followed where applicable by post hoc Tukey's or Bonferroni's multiple comparison tests. Data was analyzed using GraphPad Prism 5 (GraphPad Software, La Jolla, CA). $P < 0.05$ was considered statistically significant.

RESULTS

METH Time Dependently Increases Striatal gfap mRNA Expression

Repeated treatment with METH (5 mg/kg × 4) resulted in significant increases in the transcriptional upregulation of GFAP. As shown in Figure 1, two-way ANOVA revealed that METH caused time-dependent increases in *gfap* mRNA expression ($p < 0.0001$ for

time, treatment and their interaction). Bonferroni's post hoc tests revealed that METH treatment significantly increased *gfap* expression 12 and 24 h post-treatment ($t = 3.97$, $p < 0.01$ and $t = 7.66$, $p < 0.001$, respectively).

SN79 Treatment Blocks METH-Induced Astrogliosis

Treatment with SN79 mitigated METH-induced increases in *gfap* expression at 12 and 24 h post-treatment. One-way ANOVA revealed significant differences between treatment groups at 12 h ($F[3,38] = 16.20$, $p < 0.0001$). Tukey's post hoc multiple comparison analysis revealed a significant difference between Saline/Saline and Saline/METH treated animals ($q = 8.50$, $p < 0.001$), similar to the results obtained during the time course experiment described above. SN79 pretreatment attenuated METH-induced increases of *gfap* expression at 12 h post-treatment ($q = 7.28$, $p < 0.001$) (Figure 2A). Furthermore, one-way ANOVA revealed significant differences between treatment groups at 24 h post-treatment ($F[3,39] = 18.25$, $p < 0.0001$). Post hoc Tukey's multiple comparison tests revealed that METH treatment resulted in a significant increase in striatal *gfap* mRNA expression compared to control ($q = 9.19$, $p < 0.001$), an effect that was mitigated by treatment with SN79 ($q = 6.99$, $p < 0.001$) (Figure 2B).

Similar results were obtained through protein level analysis utilizing immunohistochemistry. METH treatment (5 mg/kg × 4) resulted in astrogliosis 72 h post-treatment. One-way ANOVA revealed differences between treatment groups in the number of reactive astrocytes within the striatum ($F[3,19] = 27.75$, $p < 0.0001$). Tukey's multiple comparison tests revealed that METH significantly increased reactive astrocytes as compared to control ($q = 10.99$, $p < 0.001$). This effect was mitigated by treatment with SN79, indicative of a blockade of METH-induced reactive astrogliosis ($q = 8.00$, $p < 0.001$) (data not shown).

Similar results were obtained through protein level analysis utilizing immunofluorescence techniques (Figure 3A). One way ANOVA revealed differences between groups in striatal intensity of GFAP immunoreactivity 72 h post-treatment ($F[3,19] = 10.07$, $p < 0.001$). Tukey's post hoc analysis revealed that, as expected, METH treatment significantly increased the striatal intensity of GFAP immunofluorescence as compared to saline-treated controls ($q = 6.67$, $p < 0.01$). SN79 treatment mitigated METH-induced increases in striatal GFAP immunofluorescence ($q = 5.69$, $p < 0.01$) (Figure 3B).

SN79 Treatment Mitigates METH-Induced Increases in OSMR Expression

METH treatment increased striatal mRNA *osmr* expression at 12 and 24 h. One-way ANOVA revealed significant differences in *osmr* mRNA expression between treatment groups at 12 h post-treatment ($F[3,38] = 36.06$, $p < 0.0001$). Post hoc Tukey's analysis showed that METH significantly increased striatal *osmr* expression as compared to saline-treated animals ($q = 12.94$, $p < 0.001$). This effect was mitigated by SN79 treatment ($q = 9.74$, $p < 0.001$) (Figure 4A). Similar effects were seen at 24 h post-treatment. One-way ANOVA revealed differences in *osmr* expression between treatment groups ($F[3,39] = 27.49$, $p < 0.0001$). Tukey's multiple comparison tests revealed that METH treatment increased *osmr* expression as compared to saline ($q = 11.26$, $p < 0.001$), an effect that was mitigated by SN79 treatment ($q = 8.92$, $p < 0.001$) (Figure 4B).

To determine if increases in OSMR expression are occurring specifically in astrocytes located within the striatum, immunofluorescence studies were conducted to qualitatively determine the level of OSMR protein between treatment groups, and the specific colocalization of increases in OSMR expression to astrocytes. One-way ANOVA revealed significant differences in the intensity of OSMR immunofluorescence at 72 h post-treatment ($F[3,19] = 11.74$, $p < 0.001$). Post hoc analysis using Tukey's multiple comparison tests showed that METH treatment increased the intensity of OSMR immunofluorescence compared to saline-treated controls ($q = 7.63$, $p < 0.001$), indicative of an increase in protein expression in agreement with earlier increases found in *osmr* mRNA expression. SN79 treatment blocked METH-induced increases in the intensity of OSMR immunofluorescence ($q = 5.89$, $p < 0.01$) (Figure 5A).

Importantly, as shown in Figure 5B, increases in GFAP and OSMR induced by METH were colocalized specifically to astrocytes within the striatum. METH induced increases in the immunoreactivity of OSMR were found to be specifically in GFAP-labelled astrocytes, an effect that was blocked by SN79 treatment. Figure 5C represents the Pearson's correlation between increases in OSMR immunofluorescence and increases in GFAP immunofluorescence, indicative of a specific increase in OSMR immunoreactivity within striatal astrocytes.

SN79 Treatment Blocks METH-Induced Phosphorylation of STAT3

Western blotting of bilateral striatal tissue 12 h post-treatment was conducted to determine the effect of METH on the phosphorylation of STAT3 (Tyr-705) and total STAT3 levels that has previously been linked to astrocyte activation by neurotoxicants, including METH *in vivo* (Hebert and O'Callaghan 2000; Sriram et al. 2004). One-way ANOVA revealed significant differences in pSTAT3 levels between groups ($F[3,31] = 5.69$, $p < 0.01$). Tukey's post hoc analysis revealed that METH treatment significantly increased the phosphorylation of STAT3 as compared to saline-treated controls at 12 h ($q = 4.90$, $p < 0.01$). SN79 treatment blocked the METH-induced phosphorylation of STAT3 ($q = 4.34$, $p < 0.05$) (Figure 6A). Conversely, there were no significant differences found in total STAT3 levels in the striatum between any of the treatment groups (one-way ANOVA, n.s.) (Figure 6B).

SN79 Treatment Attenuates METH-Induced Degeneration in the Striatum

One-way ANOVA revealed significant differences in the number of degenerating cells within the striatum between treatment groups 72 h post-treatment ($F[3,19] = 11.96$, $p < 0.001$), as determined by Fluoro-Jade B staining. METH treatment significantly increased the number of degenerating cells in the striatum as compared to saline-treated controls (Tukey's post hoc analysis, $q = 8.12$, $p < 0.001$). SN79 treatment mitigated METH-induced increases in cellular degeneration ($q = 5.20$, $p < 0.01$) (Figure 7B).

SN79 Treatment Attenuates METH-Induced Hyperthermia

Two-way ANOVA revealed significant differences in core body temperature between treatment groups, time point and their interaction ($p < 0.0001$, for treatment, time and their interaction). Bonferroni's post hoc tests revealed that METH treatment significantly increased core body temperature compared to saline-treated controls at time points 3 and 4 (t

= 4.28, $p < 0.001$ and $t = 5.85$, $p < 0.001$, respectively). Treatment with SN79 attenuated METH-induced increases in core body temperature at time points 3 and 4 ($t = 7.58$, $p < 0.001$ and $t = 8.52$, $p < 0.001$, respectively), while having no effects on its own compared to saline-treated controls ($t = 0.04$, 0.22, 0.07, 1.10 and $p > 0.05$, for time points 1 through 4, respectively).

DISCUSSION

The current study provides evidence that the sigma receptor antagonist and potential drug development candidate, SN79, mitigates METH-induced astrogliosis and degeneration in the striatum. Additionally, the current study provides evidence that the ability of SN79 to attenuate METH-induced astrogliosis is mediated through a blockade of STAT3 phosphorylation initiated by OSMR signaling.

Our findings are consistent with earlier reports that METH-induced activation of astrocytes involves OSM interactions with OSMR and subsequent induction of JAK2/STAT3 signaling (Chen and Benveniste 2004; Hebert and O'Callaghan 2000; Heinrich et al. 2003). This induction of STAT3 phosphorylation through IL-6-type signaling can result in a variety of genetic changes, including increases in GFAP expression that are associated with astrocyte activation (Hebert and O'Callaghan 2000; Oliva et al. 2012; Sriram et al. 2004; Zhong et al. 1994). The current study is the first to show that treatment with a sigma receptor antagonist mitigates METH-induced increases in signaling through this pathway and thereby counteracts METH-induced astrogliosis.

The precise mechanism(s) by which SN79 modulates this pathway has yet to be fully elucidated. It is possible that SN79 is blocking METH-induced increases in OSM, thereby leading to a reduction of signaling through OSMR. A number of labs have shown that METH treatment results in an increase in striatal expression levels of *osm* mRNA (Cadet et al. 2002; Kelly et al. 2012; Kuhn et al. 2006). Furthermore, we have also shown that SN79 mitigates METH-induced increases in striatal *osm* mRNA expression (Robson et al. 2013). This could lead to a blockade of METH-induced STAT3 phosphorylation by decreasing signaling specifically through OSMR in astrocytes and leading ultimately to a reduction in METH-induced GFAP upregulation and astrogliosis as seen in the current study.

Another potential explanation is that sigma receptor modulation within astrocytes is having an effect downstream of OSMR on STAT3 phosphorylation directly. Sigma receptors themselves and sigma receptor ligands have previously been shown to modulate the function of astrocytes *in vitro* (Ruscher et al. 2011). Furthermore, sigma receptor ligands have been shown to modulate protein expression within cultured astrocytes (Prezzavento et al. 2007), in addition to dose-dependently blocking reductions in astrocytic ATP resulting from hypoxia *in vitro* (Klouz et al. 2003). It is thus possible that sigma receptors within astrocytes are altering astrocytic responses to CNS insults that result in astrogliosis.

Another possible explanation as to how SN79 treatment is attenuating METH-induced STAT3 phosphorylation and astrogliosis is through a blockade of METH-induced dopaminergic neurotoxicity. A blockade of dopaminergic neurotoxicity has been shown to

mitigate neurotoxicant-induced astrocytic STAT3 phosphorylation, indicating a lack of astrocyte activation in the absence of dopaminergic damage (Sriram et al. 2004). Previous studies have shown that SN79 mitigates METH-induced dopaminergic and serotonergic neurotoxicity (Kaushal et al. 2013), effects that could result in the reduction of striatal STAT3 phosphorylation and subsequent astrogliosis.

One particular protein involved in the negative feedback of STAT3 signaling in astrocytes is suppressor of cytokine signaling 3 (SOCS3) (Baker et al. 2008). Astrocytic OSM signaling results in an upregulation of SOCS3 thereby suppressing the inflammatory actions of OSM, including the phosphorylation of STAT3 (Baker et al. 2008). Although SN79 treatment was found to mitigate METH-induced increases in STAT3 phosphorylation, it may be possible that modulation of ERK1/2 and JNK pathways are contributing to increases in SOCS3 (Baker et al. 2008), thereby leading to the blockade of STAT3 phosphorylation seen in the current report. Supporting this hypothesis are previous studies showing the modulation of ERK1/2 and JNK signaling by various sigma receptor ligands (Cantarella et al. 2007; Nishimura et al. 2008; Son and Kwon 2010; Tan et al. 2010; Tuerxun et al. 2010), although their effects specifically within astrocytes on these signaling pathways are currently unknown.

Our study provides evidence that METH-induced STAT3 phosphorylation occurs prior to the induction of increases in GFAP and OSMR expression elicited by METH. Previous studies have shown that maximal increases in GFAP post-treatment with METH occur between 48 and 72 h, indicative of a maximal increase in astrocyte activation (Hebert and O'Callaghan 2000; Kelly et al. 2012; Sriram et al. 2006). Moreover, it is known that maximal METH-induced increases in the phosphorylation of STAT3 occur prior to these effects (between 12 and 24 h) (Hebert and O'Callaghan 2000). Although protein changes in OSMR expression are protracted as compared to STAT3 phosphorylation, increases in *osm* mRNA expression that occur post-METH treatment are rapid (Kelly et al. 2012), suggesting that signaling through this receptor may result in a positive feedback loop, whereby signaling increases the expression of the receptor. In the current study, increases in *osmr* mRNA and protein elicited by METH were detected at time points corresponding to and also after the phosphorylation of STAT3, respectively. Interestingly, increases in OSMR expression also coincided with increases in GFAP mRNA and protein.

It is known that OSM signaling can alter gene expression in astrocytes in a biphasic manner. Although the specificity of STAT3 signaling in mediating these genetic alterations has yet to be confirmed (Van Wagoner et al. 2000), the second portion of this biphasic response has been reported to require de novo protein synthesis (Van Wagoner et al. 2000), indicating that the genetic alterations elicited through this pathway (such as increases in *gfap* mRNA expression) may require increased expression of specific proteins, including OSMR. This biphasic response could potentially be a manifestation of a positive feedback loop resulting in further increases in OSMR/gp130 signaling and increases in GFAP expression/astrocyte activation (Nakashima et al. 1999). The mitigation of METH-induced increases in astrocytic OSMR by SN79 treatment could result in a blockade of the second half of this biphasic response, thereby shunting increases in GFAP expression elicited through OSMR/gp130 signaling.

In addition to a potential role in neurotoxicity, astrocytes themselves are hypothesized to be involved in synaptic plasticity and may play large roles in the control of synaptic activity (Nedergaard and Verkhratsky 2012; Ullian et al. 2004). Substantial evidence points to astrocytes being involved in many aspects of synapse formation, maintenance and stability and they may be involved in activity-dependent synapse formation (Ullian et al. 2004). These effects are hypothesized to be involved in the actions of several drugs of abuse including METH and the modulation of astrocytes is believed to represent a novel target for the production of pharmacotherapies aimed at treating drug abuse (Cooper et al. 2012; Miguel-Hidalgo 2009; Narita et al. 2008; Rolan et al. 2009).

Previous reports have shown that METH-induced astrocyte activation is associated with METH-induced behavioral sensitization, a behavioral assay believed to be associated with neuroplastic changes elicited by drugs of abuse (Chen et al. 2009; Narita et al. 2006; Narita et al. 2005; Narita et al. 2008). Interestingly, sigma receptor ligands have previously been shown to block the development and expression of behavioral sensitization to psychostimulants, including METH (Seminerio et al. 2012b; Ujike et al. 1992; Ujike et al. 1996; Xu et al. 2010); however, whether this effect is associated with astrocyte activation has yet to be determined.

It should be noted that currently, there are no available pharmacologic agents targeting OSMR specifically and these results await confirmation through the use of genetic manipulations to conclusively confirm that OSMR signaling is specifically involved in METH-induced astrocyte activation. Sigma-1 knockout mice were also not used to confirm that the effects of SN79 specifically involve these receptors because METH is known to retain its locomotor stimulatory effects in these mice (Fontanilla et al. 2009), presumably due to compensatory actions through other systems including sigma-2 receptors. This is consistent with reports across a range of studies that suggest that the actions of METH through sigma receptors involve both the sigma-1 and sigma-2 receptor subtypes (Kaushal and Matsumoto, 2011).

SN79, the particular sigma ligand used during the current study, has been utilized previously to study the role of sigma receptors in the actions of psychostimulants such as METH (Kaushal et al. 2011a; Kaushal et al. 2013). Moreover, it produces similar protective effects as other more selective sigma ligands such as AC927 and CM156 in mitigating a number of earlier studied METH-induced endpoints (Kaushal et al. 2011b; Seminerio et al. 2011). Additionally, SN79 represents a potential drug development candidate aimed at treating the negative side effects of METH abuse such as neurotoxicity, as it has not only desirable pharmacologic effects, but also desirable pharmacokinetic parameters as well (Kaushal et al. 2011a). These effects of SN79, combined with its ability to mitigate METH-induced astrocyte activation, STAT3 phosphorylation and cellular degeneration in the striatum as described within the current study make it a viable lead for future drug development. Future studies aimed at the further delineation of the molecular mechanisms by which SN79 mitigates the neurotoxic consequences of METH are certainly warranted.

Acknowledgments

This research was supported by grants from the National Institutes of Health (DA013978, DA023205, and NS061954). Matthew J. Robson was supported by a grant from the National Institutes of Health (T32 NS007491). Ryan C. Turner was supported by a grant from the National Institutes of Health (T32 GM081741).

REFERENCES

Ajmo CT Jr. Vernon DO, Collier L, Pennypacker KR, Cuevas J. Sigma receptor activation reduces infarct size at 24 hours after permanent middle cerebral artery occlusion in rats. Curr Neurovasc Res. 2006; 3:89–98. [PubMed: 16719792]

Anderson KJ, Fugaccia I, Scheff SW. Fluoro-jade B stains quiescent and reactive astrocytes in the rodent spinal cord. J Neurotrauma. 2003; 20:1223–31. [PubMed: 14651809]

Baker BJ, Qin H, Benveniste EN. Molecular basis of oncostatin M-induced SOCS-3 expression in astrocytes. Glia. 2008; 56:1250–62. [PubMed: 18571793]

Bolte S, Cordelieres FP. A guided tour into subcellular colocalization analysis in light microscopy. J Microsc. 2006; 224:213–32. [PubMed: 17210054]

Bowyer JF, Davies DL, Schmued L, Broening HW, Newport GD, Slikker W Jr. Holson RR. Further studies of the role of hyperthermia in methamphetamine neurotoxicity. J Pharmacol Exp Ther. 1994; 268:1571–80. [PubMed: 8138969]

Bradford MM. A rapid and sensitive method for the quantitation of microgram quantities of protein utilizing the principle of protein-dye binding. Anal Biochem. 1976; 72:248–54. [PubMed: 942051]

Cadet JL, Krasnova IN. Molecular bases of methamphetamine-induced neurodegeneration. Int Rev Neurobiol. 2009; 88:101–19. [PubMed: 19897076]

Cadet JL, McCoy MT, Ladenheim B. Distinct gene expression signatures in the striata of wild-type and heterozygous c-fos knockout mice following methamphetamine administration: evidence from cDNA array analyses. Synapse. 2002; 44:211–26. [PubMed: 11984857]

Callaghan RC, Cunningham JK, Sajeev G, Kish SJ. Incidence of Parkinson's disease among hospital patients with methamphetamine-use disorders. Mov Disord. 2010; 25:2333–9. [PubMed: 20737543]

Callaghan RC, Cunningham JK, Sykes J, Kish SJ. Increased risk of Parkinson's disease in individuals hospitalized with conditions related to the use of methamphetamine or other amphetamine-type drugs. Drug Alcohol Depend. 2012; 120:35–40. [PubMed: 21794992]

Cantarella G, Bucolo C, Di Benedetto G, Pezzino S, Lempereur L, Calvagna R, Clementi S, Pavone P, Fiore L, Bernardini R. Protective effects of the sigma agonist Pre-084 in the rat retina. Br J Ophthalmol. 2007; 91:1382–4. [PubMed: 17522150]

Chen JC, Chen PC, Chiang YC. Molecular mechanisms of psychostimulant addiction. Chang Gung Med J. 2009; 32:148–54. [PubMed: 19403004]

Chen SH, Benveniste EN. Oncostatin M: a pleiotropic cytokine in the central nervous system. Cytokine Growth Factor Rev. 2004; 15:379–91. [PubMed: 15450253]

Chen SH, Gillespie GY, Benveniste EN. Divergent effects of oncostatin M on astroglioma cells: influence on cell proliferation, invasion, and expression of matrix metalloproteinases. Glia. 2006; 53:191–200. [PubMed: 16206166]

Cooper ZD, Jones JD, Comer SD. Glial modulators: a novel pharmacological approach to altering the behavioral effects of abused substances. Expert Opin Investig Drugs. 2012; 21:169–78.

Damjanac M, Rioux Bilan A, Barrier L, Pontcharraud R, Anne C, Hugon J, Page G. Fluoro-Jade B staining as useful tool to identify activated microglia and astrocytes in a mouse transgenic model of Alzheimer's disease. Brain Res. 2007; 1128:40–9. [PubMed: 17125750]

Deng X, Wang Y, Chou J, Cadet JL. Methamphetamine causes widespread apoptosis in the mouse brain: evidence from using an improved TUNEL histochemical method. Brain Res Mol Brain Res. 2001; 93:64–9. [PubMed: 11532339]

Eisch AJ, Schmued LC, Marshall JF. Characterizing cortical neuron injury with Fluoro-Jade labeling after a neurotoxic regimen of methamphetamine. Synapse. 1998; 30:329–33. [PubMed: 9776136]

Fontanilla D, Johannessen M, Hajipour AR, Cozzi NV, Jackson MB, Ruoho AE. The hallucinogen N,N-dimethyltryptamine (DMT) is an endogenous sigma-1 receptor regulator. Science. 2009; 323:934–7. [PubMed: 19213917]

Hebert MA, O'Callaghan JP. Protein phosphorylation cascades associated with methamphetamine-induced glial activation. Ann N Y Acad Sci. 2000; 914:238–62. [PubMed: 11085325]

Heinrich PC, Behrmann I, Haan S, Hermanns HM, Muller-Newen G, Schaper F. Principles of interleukin (IL)-6-type cytokine signalling and its regulation. Biochem J. 2003; 374:1–20. [PubMed: 12773095]

Hellewell SB, Bowen WD. A sigma-like binding site in rat pheochromocytoma (PC12) cells: decreased affinity for (+)-benzomorphans and lower molecular weight suggest a different sigma receptor form from that of guinea pig brain. Brain Res. 1990; 527:244–53. [PubMed: 2174717]

Jayanthi S, Deng X, Ladenheim B, McCoy MT, Cluster A, Cai NS, Cadet JL. Calcineurin/NFAT-induced up-regulation of the Fas ligand/Fas death pathway is involved in methamphetamine-induced neuronal apoptosis. Proc Natl Acad Sci U S A. 2005; 102:868–73. [PubMed: 15644446]

Kaushal N, Robson MJ, Vinnakota H, Narayanan S, Avery BA, McCurdy CR, Matsumoto RR. Synthesis and pharmacological evaluation of 6-acetyl-3-(4-(4-(4-fluorophenyl)piperazin-1-yl)butyl)benzo[d]oxazol-2(3H)-one (SN79), a cocaine antagonist, in rodents. AAPS J. 2011 a.; 13:336–46. [PubMed: 21494909]

Kaushal N, Seminerio MJ, Robson MJ, McCurdy CR, Matsumoto RR. Pharmacological evaluation of SN79, a sigma (sigma) receptor ligand, against methamphetamine-induced neurotoxicity in vivo. Eur Neuropsychopharmacol. 2013; 23:960–971. [PubMed: 22921523]

Kaushal N, Seminerio MJ, Shaikh J, Medina MA, Mesangeau C, Wilson LL, McCurdy CR, Matsumoto RR. CM156, a high affinity sigma ligand, attenuates the stimulant and neurotoxic effects of methamphetamine in mice. Neuropharmacology. 2011b; 61:992–1000. [PubMed: 21762711]

Kelly KA, Miller DB, Bowyer JF, O'Callaghan JP. Chronic exposure to corticosterone enhances the neuroinflammatory and neurotoxic responses to methamphetamine. J Neurochem. 2012; 122:995–1009. [PubMed: 22776046]

Klouz A, Tillement JP, Boussard MF, Wierzbicki M, Berezowski V, Cecchelli R, Labidalle S, Onteniente B, Morin D. [3H]BHDP as a novel and selective ligand for sigma1 receptors in liver mitochondria and brain synaptosomes of the rat. FEBS Lett. 2003; 553:157–62. [PubMed: 14550565]

Kuhn DM, Francescutti-Verbeem DM, Thomas DM. Dopamine quinones activate microglia and induce a neurotoxic gene expression profile: relationship to methamphetamine-induced nerve ending damage. Ann N Y Acad Sci. 2006; 1074:31–41. [PubMed: 17105901]

Lau JW, Senok S, Stadlin A. Methamphetamine-induced oxidative stress in cultured mouse astrocytes. Ann N Y Acad Sci. 2000; 914:146–56. [PubMed: 11085317]

Matsumoto RR, Shaikh J, Wilson LL, Vedam S, Coop A. Attenuation of methamphetamine-induced effects through the antagonism of sigma (sigma) receptors: Evidence from in vivo and in vitro studies. Eur Neuropsychopharmacol. 2008; 18:871–81. [PubMed: 18755577]

Miguel-Hidalgo JJ. The role of glial cells in drug abuse. Curr Drug Abuse Rev. 2009; 2:72–82. [PubMed: 19630738]

Nakashima K, Wiese S, Yanagisawa M, Arakawa H, Kimura N, Hisatsune T, Yoshida K, Kishimoto T, Sendtner M, Taga T. Developmental requirement of gp130 signaling in neuronal survival and astrocyte differentiation. J Neurosci. 1999; 19:5429–34. [PubMed: 10377352]

Narita M, Miyatake M, Shibasaki M, Shindo K, Nakamura A, Kuzumaki N, Nagumo Y, Suzuki T. Direct evidence of astrocytic modulation in the development of rewarding effects induced by drugs of abuse. Neuropsychopharmacology. 2006; 31:2476–88. [PubMed: 16407899]

Narita M, Miyatake M, Shibasaki M, Tsuda M, Koizumi S, Yajima Y, Inoue K, Suzuki T. Long-lasting change in brain dynamics induced by methamphetamine: enhancement of protein kinase C-dependent astrocytic response and behavioral sensitization. J Neurochem. 2005; 93:1383–92. [PubMed: 15935054]

Narita M, Suzuki M, Kuzumaki N, Miyatake M, Suzuki T. Implication of activated astrocytes in the development of drug dependence: differences between methamphetamine and morphine. Ann N Y Acad Sci. 2008; 1141:96–104. [PubMed: 18991953]

Nedergaard M, Verkhratsky A. Artifact versus reality--how astrocytes contribute to synaptic events. Glia. 2012; 60:1013–23. [PubMed: 22228580]

Nguyen EC, McCracken KA, Liu Y, Pouw B, Matsumoto RR. Involvement of sigma (sigma) receptors in the acute actions of methamphetamine: receptor binding and behavioral studies. Neuropharmacology. 2005; 49:638–45. [PubMed: 15939443]

Nishimura T, Ishima T, Iyo M, Hashimoto K. Potentiation of nerve growth factor-induced neurite outgrowth by fluvoxamine: role of sigma-1 receptors, IP3 receptors and cellular signaling pathways. PLoS One. 2008; 3:e2558. [PubMed: 18596927]

O'Callaghan JP, Miller DB. Neurotoxicity profiles of substituted amphetamines in the C57BL/6J mouse. J Pharmacol Exp Ther. 1994; 270:741–51. [PubMed: 8071867]

O'Callaghan JP, Sriram K. Focused microwave irradiation of the brain preserves in vivo protein phosphorylation: comparison with other methods of sacrifice and analysis of multiple phosphoproteins. J Neurosci Methods. 2004; 135:159–68. [PubMed: 15020100]

Oliva AA Jr. Kang Y, Sanchez-Molano J, Furones C, Atkins CM. STAT3 signaling after traumatic brain injury. J Neurochem. 2012; 120:710–20. [PubMed: 22145815]

Prezzavento O, Campisi A, Ronsisvalle S, Li Volti G, Marrazzo A, Bramanti V, Cannavo G, Vanella L, Cagnotto A, Mennini T. Novel sigma receptor ligands: synthesis and biological profile. J Med Chem. 2007; 50:951–61. others. [PubMed: 17328523]

Pu C, Fisher JE, Cappon GD, Vorhees CV. The effects of amfonelic acid, a dopamine uptake inhibitor, on methamphetamine-induced dopaminergic terminal degeneration and astrocytic response in rat striatum. Brain Res. 1994; 649:217–24. [PubMed: 7953636]

Raivich G, Bohatschek M, Kloss CU, Werner A, Jones LL, Kreutzberg GW. Neuroglial activation repertoire in the injured brain: graded response, molecular mechanisms and cues to physiological function. Brain Res Brain Res Rev. 1999; 30:77–105. [PubMed: 10407127]

Reichel CM, Ramsey LA, Schwendt M, McGinty JF, See RE. Methamphetamine-induced changes in the object recognition memory circuit. Neuropharmacology. 2012; 62:1119–26. [PubMed: 22115899]

Robson MJ, Turner RC, Naser ZJ, McCurdy CR, Huber JD, Matsumoto RR. SN79, a sigma receptor ligand, blocks methamphetamine-induced microglial activation and cytokine upregulation. Exp Neurol. 2013

Rolan P, Hutchinson M, Johnson K. Ibudilast: a review of its pharmacology, efficacy and safety in respiratory and neurological disease. Expert Opin Pharmacother. 2009; 10:2897–904. [PubMed: 19929708]

Romanelli F, Smith KM. Clinical effects and management of methamphetamine abuse. Pharmacotherapy. 2006; 26:1148–56. [PubMed: 16863490]

Ruscher K, Shamloo M, Rickhag M, Ladunga I, Soriano L, Gisselsson L, Toresson H, Ruslim-Litrus L, Oksenberg D, Urfer R. The sigma-1 receptor enhances brain plasticity and functional recovery after experimental stroke. Brain. 2011; 134:732–46. others. [PubMed: 21278085]

Schmitz C, Hof PR. Design-based stereology in neuroscience. Neuroscience. 2005; 130:813–31. [PubMed: 15652981]

Schmued LC, Hopkins KJ. Fluoro-Jade: novel fluorochromes for detecting toxicant-induced neuronal degeneration. Toxicol Pathol. 2000; 28:91–9. [PubMed: 10668994]

Schwendt M, Rocha A, See RE, Pacchioni AM, McGinty JF, Kalivas PW. Extended methamphetamine self-administration in rats results in a selective reduction of dopamine transporter levels in the prefrontal cortex and dorsal striatum not accompanied by marked monoaminergic depletion. J Pharmacol Exp Ther. 2009; 331:555–62. [PubMed: 19648469]

Seminerio MJ, Hansen R, Kaushal N, Zhang HT, McCurdy CR, Matsumoto RR. The evaluation of AZ66, an optimized sigma receptor antagonist, against methamphetamine-induced dopaminergic neurotoxicity and memory impairment in mice. Int J Neuropsychopharmacol. 2012a:1–12.

Seminerio MJ, Kaushal N, Shaikh J, Huber JD, Coop A, Matsumoto RR. Sigma (sigma) receptor ligand, AC927 (N-phenethylpiperidine oxalate), attenuates methamphetamine-induced

hyperthermia and serotonin damage in mice. Pharmacol Biochem Behav. 2011; 98:12–20. [PubMed: 21130800]

Seminerio MJ, Robson MJ, Abdelazeem AH, Mesangeau C, Jamalapuram S, Avery BA, McCurdy CR, Matsumoto RR. Synthesis and pharmacological characterization of a novel sigma receptor ligand with improved metabolic stability and antagonistic effects against methamphetamine. AAPS J. 2012b; 14:43–51. [PubMed: 22183188]

Smith DW, Bailes JE, Fisher JA, Robles J, Turner RC, Mills JD. Internal jugular vein compression mitigates traumatic axonal injury in a rat model by reducing the intracranial slosh effect. Neurosurgery. 2012; 70:740–6. [PubMed: 21904255]

Son JS, Kwon YB. Sigma-1 receptor antagonist BD1047 reduces allodynia and spinal ERK phosphorylation following chronic compression of dorsal root ganglion in rats. Korean J Physiol Pharmacol. 2010; 14:359–64. [PubMed: 21311675]

Sriram K, Benkovic SA, Hebert MA, Miller DB, O'Callaghan JP. Induction of gp130-related cytokines and activation of JAK2/STAT3 pathway in astrocytes precedes up-regulation of glial fibrillary acidic protein in the 1-methyl-4-phenyl-1,2,3,6-tetrahydropyridine model of neurodegeneration: key signaling pathway for astrogliosis in vivo? J Biol Chem. 2004; 279:19936–47. [PubMed: 14996842]

Sriram K, Miller DB, O'Callaghan JP. Minocycline attenuates microglial activation but fails to mitigate striatal dopaminergic neurotoxicity: role of tumor necrosis factor-alpha. J Neurochem. 2006; 96:706–18. [PubMed: 16405514]

Stadlin A, Lau JW, Szeto YK. A selective regional response of cultured astrocytes to methamphetamine. Ann N Y Acad Sci. 1998; 844:108–21. [PubMed: 9668669]

Tan F, Guio-Aguilar PL, Downes C, Zhang M, O'Donovan L, Callaway JK, Crack PJ. The sigma 1 receptor agonist 4-PPBP elicits ERK1/2 phosphorylation in primary neurons: a possible mechanism of neuroprotective action. Neuropharmacology. 2010; 59:416–24. [PubMed: 20538010]

Thomas DM, Francescutti-Verbeem DM, Liu X, Kuhn DM. Identification of differentially regulated transcripts in mouse striatum following methamphetamine treatment--an oligonucleotide microarray approach. J Neurochem. 2004; 88:380–93. [PubMed: 14690526]

Todd G, Noyes C, Flavel SC, Della Vedova CB, Spyropoulos P, Chatterton B, Berg D, White JM. Illicit stimulant use is associated with abnormal substantia nigra morphology in humans. PLoS One. 2013; 8:e56438. [PubMed: 23418568]

Tuerxun T, Numakawa T, Adachi N, Kumamaru E, Kitazawa H, Kudo M, Kunugi H. SA4503, a sigma-1 receptor agonist, prevents cultured cortical neurons from oxidative stress-induced cell death via suppression of MAPK pathway activation and glutamate receptor expression. Neurosci Lett. 2010; 469:303–8. [PubMed: 20025928]

Turner RC, Naser ZJ, Bailes JE, Smith DW, Fisher JA, Rosen CL. Effect of slosh mitigation on histologic markers of traumatic brain injury: laboratory investigation. J Neurosurg. 2012; 117:1110–8. [PubMed: 22998060]

Ujike H, Kanzaki A, Okumura K, Akiyama K, Otsuki S. Sigma antagonist BMY 14802 prevents methamphetamine-induced sensitization. Life Sci. 1992; 50:PL129–34. [PubMed: 1313134]

Ujike H, Kuroda S, Otsuki S. Sigma receptor antagonists block the development of sensitization to cocaine. Eur J Pharmacol. 1996; 296:123–8. [PubMed: 8838447]

Ullian EM, Christopherson KS, Barres BA. Role for glia in synaptogenesis. Glia. 2004; 47:209–16. [PubMed: 15252809]

Van Wagoner NJ, Benveniste EN. Interleukin-6 expression and regulation in astrocytes. J Neuroimmunol. 1999; 100:124–39. [PubMed: 10695723]

Van Wagoner NJ, Choi C, Repovic P, Benveniste EN. Oncostatin M regulation of interleukin-6 expression in astrocytes: biphasic regulation involving the mitogen-activated protein kinases ERK1/2 and p38. J Neurochem. 2000; 75:563–75. [PubMed: 10899931]

Volkow ND, Chang L, Wang GJ, Fowler JS, Franceschi D, Sedler M, Gatley SJ, Miller E, Hitzemann R, Ding YS. Loss of dopamine transporters in methamphetamine abusers recovers with protracted abstinence. J Neurosci. 2001a; 21:9414–8. others. [PubMed: 11717374]

Volkow ND, Chang L, Wang GJ, Fowler JS, Leonido-Yee M, Franceschi D, Sedler MJ, Gatley SJ, Hitzemann R, Ding YS. Association of dopamine transporter reduction with psychomotor impairment in methamphetamine abusers. Am J Psychiatry. 2001b; 158:377–82. others. [PubMed: 11229977]

Xu YT, Kaushal N, Shaikh J, Wilson LL, Mesangeau C, McCurdy CR, Matsumoto RR. A novel substituted piperazine, CM156, attenuates the stimulant and toxic effects of cocaine in mice. J Pharmacol Exp Ther. 2010; 333:491–500. [PubMed: 20100904]

Zamanian JL, Xu L, Foo LC, Nouri N, Zhou L, Giffard RG, Barres BA. Genomic analysis of reactive astrogliosis. J Neurosci. 2012; 32:6391–410. [PubMed: 22553043]

Zhong Z, Wen Z, Darnell JE Jr. Stat3: a STAT family member activated by tyrosine phosphorylation in response to epidermal growth factor and interleukin-6. Science. 1994; 264:95–8. [PubMed: 8140422]

Highlights

- Neurotoxic methamphetamine (METH) causes astrogliosis in the striatum.
- METH also increases astrocytic OSMR and pSTAT3 expression.
- SN79, a σ receptor antagonist, mitigates these METH-induced changes in astrocytes.
- Neurotoxic METH also induces striatal cell degeneration which can be mitigated by SN79.
- σ receptors can be targeted to attenuate METH-induced changes in astrocytes following neurotoxic exposures.

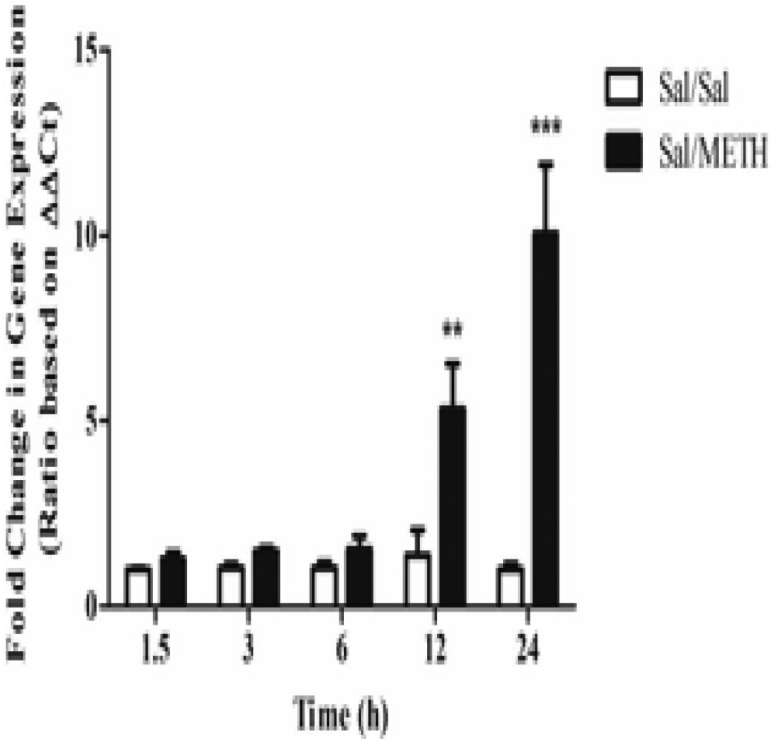

Figure 1.

METH (5 mg/kg x 4) treatment resulted in time-dependent increases in striatal *gfap* mRNA expression. METH was found to significantly increase *gfap* expression at both 12 and 24 h post-treatment. Two-way ANOVA, followed by post hoc Bonferroni's multiple comparison tests. n=5/group. **$p < 0.01$, ***$p < 0.001$, Sal/METH vs. Sal/Sal

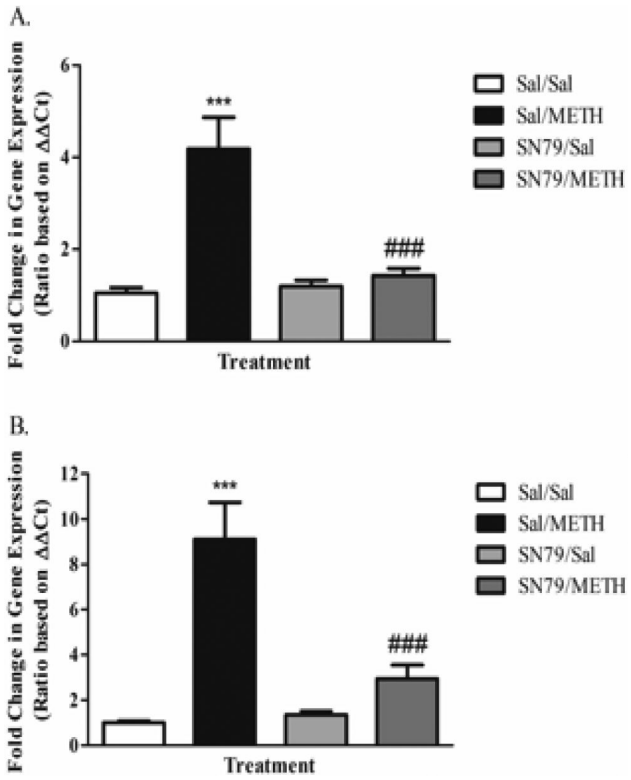

Figure 2.

Treatment with SN79 was found to attenuate METH-induced increases in striatal *gfap* mRNA expression at both 12 (A) and 24 h (B), indicating a blockade of astrocyte activation. One-way ANOVA, followed by post hoc Tukey's multiple comparison tests. n=10/group. ***$p < 0.001$, Sal/METH vs. Sal/Sal; ###$p < 0.001$, SN79/METH vs. Sal/METH

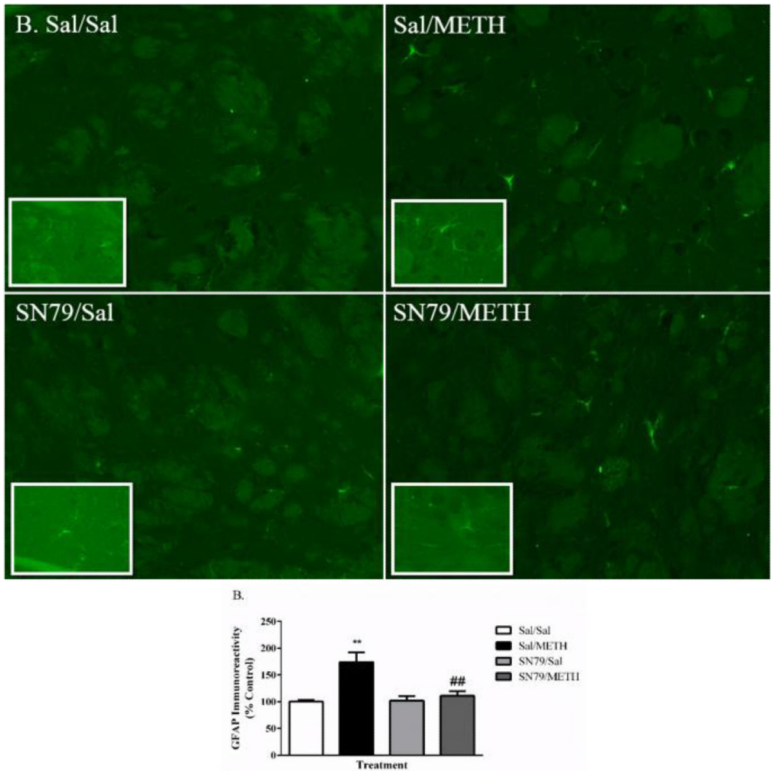

Figure 3.

SN79 mitigates METH-induced increases in striatal GFAP immunoreactivity. METH (5 mg/kg x 4) resulted in significant increases in GFAP immunofluorescence. This effect was blocked by SN79 (3 mg/kg × 4) treatment. (A) Qualitative images of GFAP immunoreactivity in response to METH and blockade by SN79 treatment. Clockwise from top left: Sal/Sal, Sal/METH, SN79/METH, SN79/Sal. Large images = 20×; Inset images = 63×. (B) Quantification of the attenuation of METH-induced increases in GFAP immunoreactivity by SN79 treatment. One-way ANOVA, followed by post hoc Tukey's multiple comparison tests. n=5/group, 3 slices/brain averaged for each data point. **p < 0.01, Sal/METH vs. Sal/Sal; ##p < 0.01, SN79/METH vs. Sal/METH

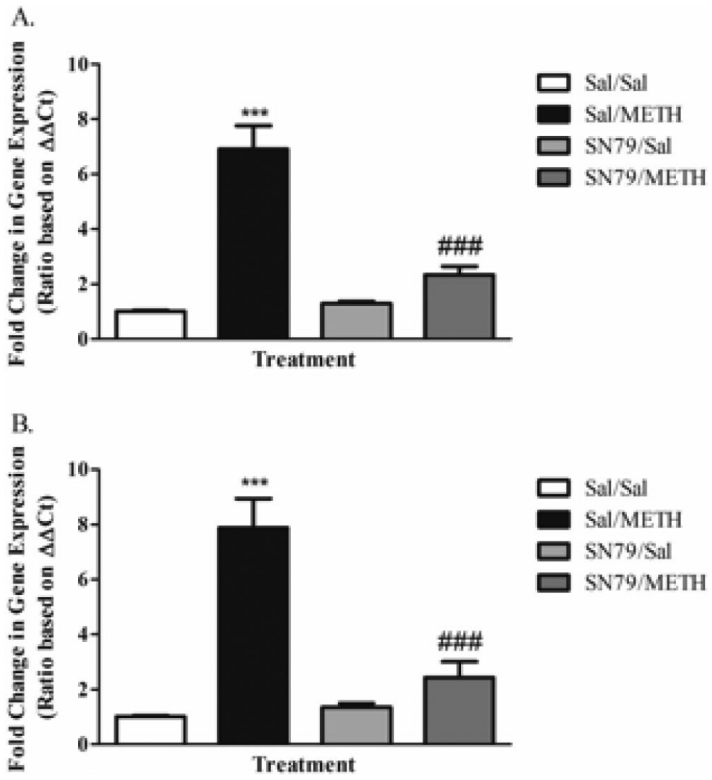

Figure 4.

SN79 (3 mg/kg × 4) treatment blocks METH-induced (5 mg/kg × 4) increases in striatal *osmr* mRNA expression at 12 (A) and 24 h (B). One-way ANOVA, followed by post hoc Tukey's multiple comparison tests. n=10/group. ***p < 0.001, Sal/METH vs. Sal/Sal; ###p < 0.001, SN79/METH vs. Sal/METH

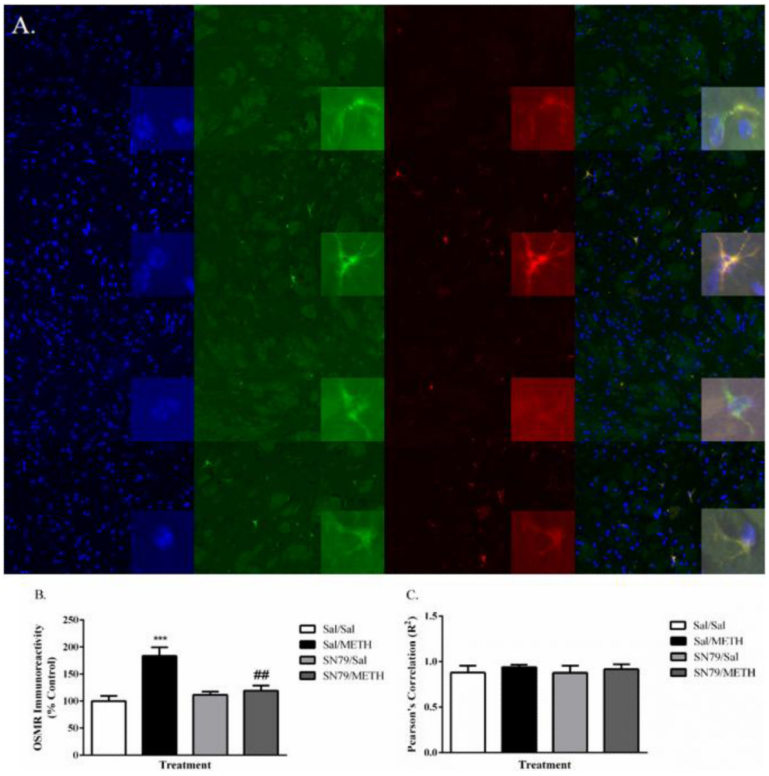

Figure 5.

(A) METH treatment increased OSMR immunoreactivity in the striatum, an effect mitigated by SN79 treatment. One-way ANOVA, followed by post hoc Tukey's multiple comparison tests. n=5/group, 3 slices/brain averaged for each data point. **p < 0.01, ***p< 0.001, Sal/METH vs. Sal/Sal; ##p < 0.01, SN79/METH vs. Sal/METH (B) Representative images showing increases in GFAP immunoreactivity, increases in astrocytic OSMR immunoreactivity and their colocalization in the striatum by treatment group. Top to bottom: Sal/Sal, Sal/METH, SN79/Sal, SN79/METH Left to right: DAPI nuclear staining, GFAP, OSMR, overlay image. Large images = 20×; Inset images = 63×. (C) Pearson's correlation of increases in OSMR immunoreactivity and increases in GFAP immunoreactivity, indicating an increase in OSMR that is specific to striatal astrocytes.

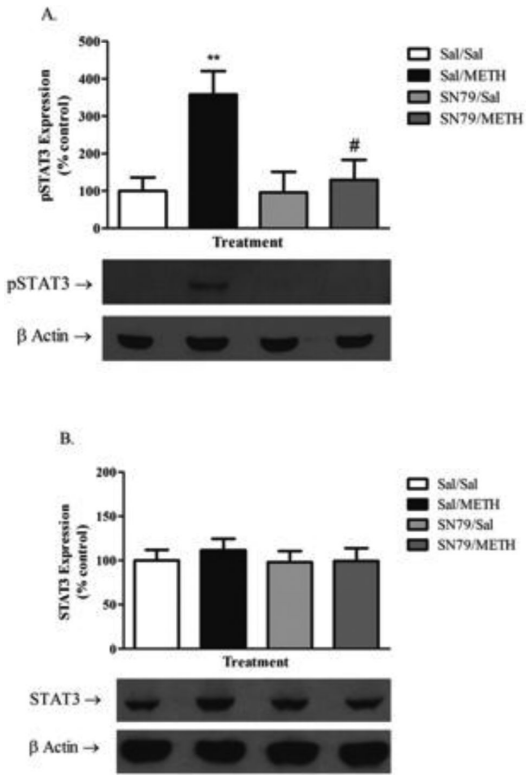

Figure 6.

SN79 mitigates METH-induced increases in the phosphorylation of STAT3 (Tyr-705). (A) METH treatment (5 mg/kg × 4) increases the phosphorylation of STAT3 (Tyr-705) at 12 h, an effect that is mitigated by treatment with SN79 (3 mg/kg × 4). One-way ANOVA followed by post hoc Tukey's multiple comparison tests. **$p < 0.01$, Sal/METH vs. Sal/Sal; #$p < 0.05$, SN79/METH vs. Sal/METH (B) No differences were detected between any of the treatment groups in total STAT3 expression.

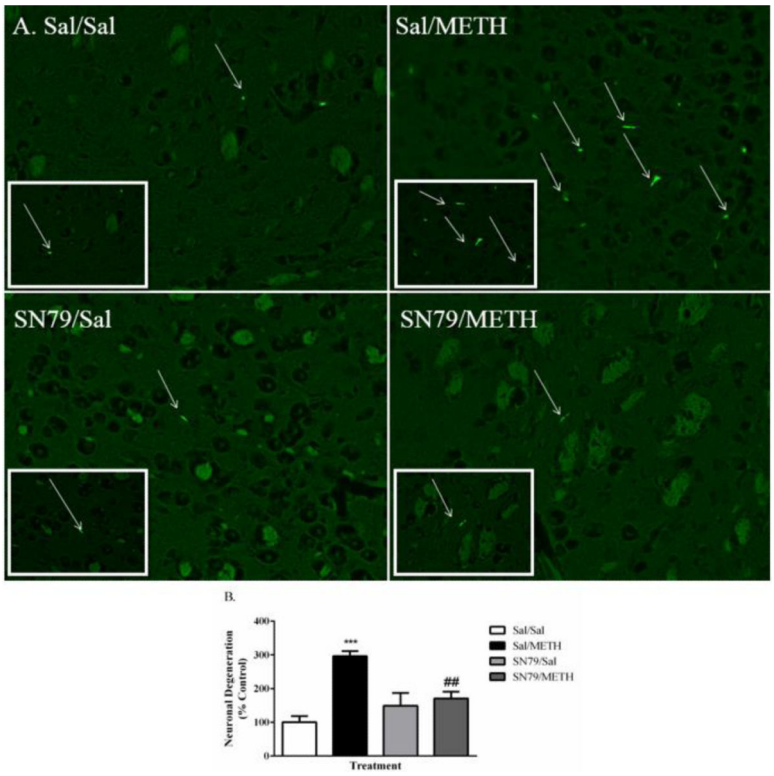

Figure 7.

SN79 (3 mg/kg × 4) treatment attenuates METH-induced (5 mg/kg × 4) neuronal degeneration in the striatum as measured by Fluoro-Jade B staining. (A) Representative images of Fluoro-Jade B labeled degenerating neurons in the striatum for each respective treatment group. Clockwise from top left: Sal/Sal, Sal/METH, SN79/METH, SN79/Sal. (B) Quantification of striatal neuronal degeneration by treatment group. One-way ANOVA, followed by post hoc Tukey's multiple comparison tests. n=5/group, 3 slices/brain averaged for each data point. ***$p < 0.001$, Sal/METH vs. Sal/Sal; ##$p < 0.01$, SN79/METH vs. Sal/METH